J. Vet. Sci. (2008), **9**(4), 387–393

JOURNAL OF
Veterinary
Science

Implantation of canine umbilical cord blood-derived mesenchymal stem cells mixed with beta-tricalcium phosphate enhances osteogenesis in bone defect model dogs

Byung-Jun Jang[1], Ye-Eun Byeon[1], Ji-Hey Lim[1], Hak-Hyun Ryu[1], Wan Hee Kim[1], Yoshihisa Koyama[3], Masanori Kikuchi[4], Kyung-Sun Kang[2,*], Oh-Kyeong Kweon[1,*]

[1]Department of Veterinary Surgery, [2]Laboratories of Stem Cell and Tumor Biology, Department of Veterinary Public Health, College of Veterinary Medicine, Seoul National University, Seoul 151-742, Korea
[3]Department of Biodesign, Institute of Biomaterials & Bioengineering, Tokyo Medical & Dental University, Tokyo, Japan
[4]Biomaterials Center, National Institute for Materials Science, Tsukuba, Japan

This study was performed to evaluate the osteogenic effect of allogenic canine umbilical cord blood-derived mesenchymal stem cells (UCB-MSCs) mixed with beta-tricalcium phosphate (β-TCP) in orthotopic implantation. Seven hundred milligrams of β-TCP mixed with 1×10^6 UCB-MSCs diluted with 0.5 ml of saline (group CM) and mixed with the same volume of saline as control (group C) were implanted into a 1.5 cm diaphyseal defect and wrapped with PLGC membrane in the radius of Beagle dogs. Radiographs of the antebrachium were made after surgery. The implants were harvested 12 weeks after implantation and specimens were stained with H&E, toluidine blue and Villanueva-Goldner stains for histological examination and histomorphometric analysis of new bone formation. Additionally, UCB-MSCs were applied to a dog with non-union fracture. Radiographically, continuity between implant and host bone was evident at only one of six interfaces in group C by 12 weeks, but in three of six interfaces in group CM. Radiolucency was found only near the bone end in group C at 12 weeks after implantation, but in the entire graft in group CM. Histologically, bone formation was observed around β-TCP in longitudinal sections of implant in both groups. Histomorphometric analysis revealed significantly increased new bone formation in group CM at 12 weeks after implantation ($p < 0.05$). When applied to the non-union fracture, fracture healing was identified by 6 weeks after injection of UCB-MSCs. The present study indicates that a mixture of UCB-MSCs and β-TCP is a promising osteogenic material for repairing bone defects.

Keywords: β-TCP, dog, mesenchymal stem cell, osteogenesis, umbilical cord blood

*Corresponding author
Tel: +82-2-880-1248; Fax: +82-2-888-2866
E-mail: ohkweon@snu.ac.kr, kangpub@snu.ac.kr

Introduction

Repairing non-union fractures or bony defects is surgically challenging. Synthetic bone substitutes and osteogenic materials have been evaluated as aids [2,18,29,31]. Among the synthetic bone substitutes, hydroxyapatite and other calcium phosphate ceramics have shown the most promising results due to their osteoconductive properties, unlimited availability and absence of immune response [9,25,28]. A potential limitation of such materials is the slow biodegradation rate observed in pure hydroxyapatite. However, implants comprised of beta-tricalcium phosphate (β-TCP) are resorbable [6]. β-TCP has shown good biocompatibility and osseointegration, but appreciable amounts were still present after 12 months [17].

Recently, it has been reported that umbilical cord blood can serve as an alternative source of mesenchymal stem cells (MSCs), and human umbilical cord blood-derived MSCs (UCB-MSCs) contain multi-potent cells including those with osteogenic potential [22,27]. Furthermore, UCB-MSCs may be immune-privileged cells with surface characteristics that enable circumvention of immune rejection [5,7]. Recently, we isolated canine UCB-MSCs [21], which provides a ready source of the cells.

The present study reports enhanced osteogenesis by the implantation of canine UCB-MSCs mixed with β-TCP in bone defect model dogs, and the successful repair of a non-union fracture case by allografting and injection of canine UCB-MSCs.

Materials and Methods

Animals

Six healthy Beagle dogs (15.4 ± 1.2 months, B.W 6~7 kg) were used for the orthotopic implantation. There were two

experimental groups: canine UCB-MSCs grafting and control, with three dogs per group. The dogs were housed in indoor cages. Food and water were supplied *ad libitum.* All animal experiments conformed to the Guidelines for Animal Experiments of Seoul National University.

Preparation of canine UCB-MSCs

Fetal umbilical cord blood was collected during Caesarean section of pregnant female dogs. Canine UCB-MSCs were produced by culturing to facilitate proliferation of mononucleated cells from cord blood as verified by fluorescence-activated cell sorting (FACS) analysis, and by the *in vitro* differentiation of bone [21]. Cells (1×10^6) were prepared for implantation. Canine UCB-MSCs were suspended with 500 μl of normal saline prior to mixing with 700 mg of β-TCP (group CM). The same volume of normal saline mixed with β-TCP was prepared as the control (group C).

Bioceramic implants

β-TCP powder and the β-TCP/poly L-lactide-co-ε-caprolactone composite (TCP/PLGC) membrane were gifts of the Biomaterials Center, National Institute for Materials Science, Japan. β-TCP particle diameter averaged about 125 μm and the molecular weight of PLGC was 250,000. Each TCP/PLGC membrane was prepared by mixing β-TCP particles and PLGC in a weight ratio of 7 : 3 for 10 min at 180°C. The composite was formed into 200 μm thick membranes with a hot-press [15].

Orthotopic implantation and harvest

After dogs were premedicated with 0.2 mg butorphanol (Myungmoon Pharm, Korea) at a dose of 0.2 mg/kg body weight and acepromazine maleate (Samwoo, Korea) at a dose of 0.05 mg/kg body weight, 1% propofol (Claris Lifesciences, India) at a dose of 6 mg/kg body weight was intravenously injected to induce anesthesia. Isoflurane (Ilsung Pharmaceutical, Korea) was used to maintain anesthesia. Under sterile conditions, a craniomedial approach was performed to expose the diaphysis of right radius. The periosteum was elevated only enough to allow the plate to lie directly on the bone. An eight-hole, 2.7 dynamic compression plate (Synthes, Switzerland) was contoured and applied to the cranial aspect of the radius. The plate was then removed and a 15 mm long osteoperiosteal segmental cortical defect was made at the mid-portion of the diaphysis with an oscillation bone saw [3]. The plate was then reapplied, mixed materials were implanted in the defect, and the implanted site was wrapped with TCP/PLGC to prevent leakage of implants. After closing the soft tissue, a Robert John's bandage was applied for 2 weeks. The implants were harvested 12 weeks after implantation.

Radiographic examination

Lateral and craniocaudal radiographs of the right antebrachium were made before and immediately after surgery as well as 2, 4, 8 and 12 weeks after implantation. Each radiographic evaluation focused on the continuity between host bone and implant, and the change of implant radiopacity.

Histological examination

Segments of bone including defect sites were removed and processed for histological analysis without decalcification. Specimens were fixed in 4% paraformaldehyde and processed for methyl methacrylate embedding using an Osteo-Bed Bone embedding kit (Polysciences, USA). Longitudinal sections were cut in the sagittal planes using a microtome. The central longitudinal sections from each radius were ground to a thickness of 100 μm and stained with hematoxylin and eosin (H&E), toluidine blue, and Villanueva-Goldner stains to evaluate new bone formation. Stained sections from each group were observed under a light microscope and were scanned using an attached digital camera and a NIS-Elements system (Nikon, Japan). The areas of new bone formation and the residual β-TCP were determined and converted to a percentage of total area of bone defect.

Statistics

Student's *t*-test was performed to compare the new bone formation between the C and CM groups at a 95% confidence level.

Clinical application

A 6-month-old Toy poodle that had been operated on twice previously presented to the Veterinary Medical Teaching

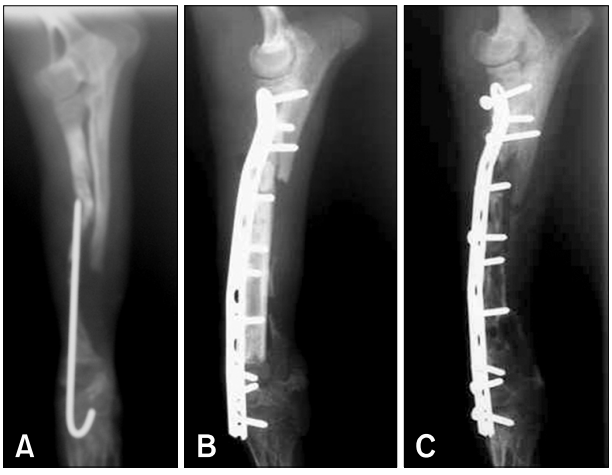

Fig. 1. Radiographs of antebrachium in clinical application. (A) Preoperative: non-union fracture of the right distal radius. (B) Postoperative: plate & screw fixation with cortical allograft and cancellous bone autograft. (C) 9 weeks postoperative: Bone lysis, irregular margin and disuse atrophy of the bone were observed.

Hospital, Seoul National University, with radial non-union fracture (Fig. 1A). A cortical allograft was implanted (Fig. 1B). Graft lysis and instability of fractured site were observed 9 weeks after implantation (Fig. 1C). Under fluoroscopy-aided guidance, 1×10^7 canine UCB- MSCs diluted with 0.5 ml saline were injected into the bone defect formed by graft lysis. Another injection was done 1 month later.

Results

Animal model

All dogs were able to bear weight partially by 2 weeks, after which they became active in their enclosures. All wounds healed without infection and there were no failures of fixation.

Radiographic findings

Postoperatively, the defect could be visualized easily because of the radiopacity of the material. With time, the radiolucent site gradually expanded from interface between the host bone and the implant to the central part of the defect in both groups, but the tendency was clearer in group CM (Fig. 2). Radiolucency was found only near the bone end in group C by 12 weeks but was evident throughout the entire graft in group CM.

Union between implant and host bone was seen at only one of six interfaces in group C by 12 weeks (Fig. 2: proximal interface of C1). In group CM, continuity was established at three of six interfaces by 12 weeks (Fig. 2: proximal interface of CM1, 2 and 3).

Histological findings

Bone formation was observed around β-TCP in longitudinal

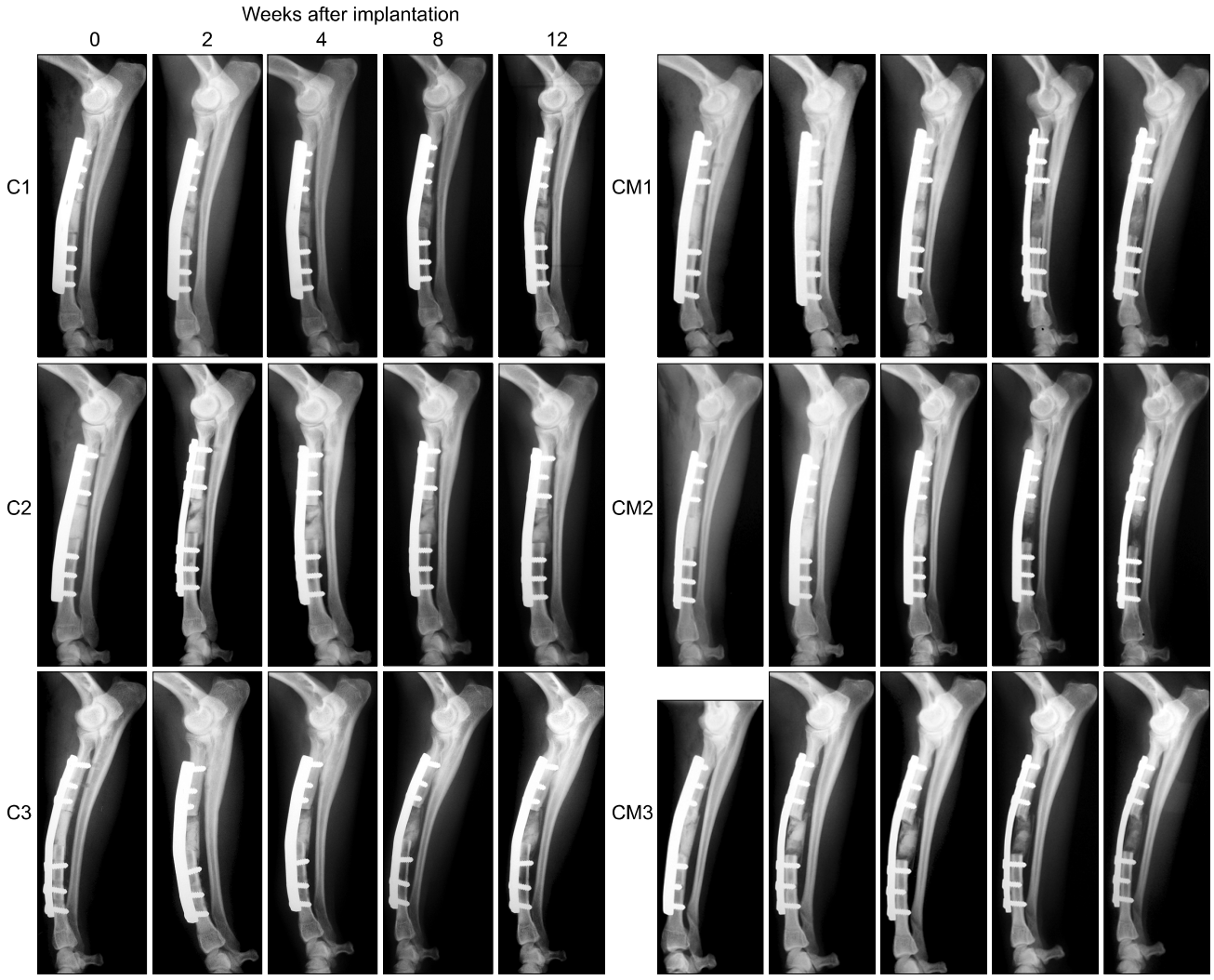

Fig. 2. Lateral radiographs of antebrachium after implantation and 2, 4, 8, 12 weeks. Radiolucency is found only near bone end in group C (implantation of β-TCP with saline), but entire graft in group CM (implantation of β-TCP with umbilical cord blood derived stem cells) at 12 weeks.

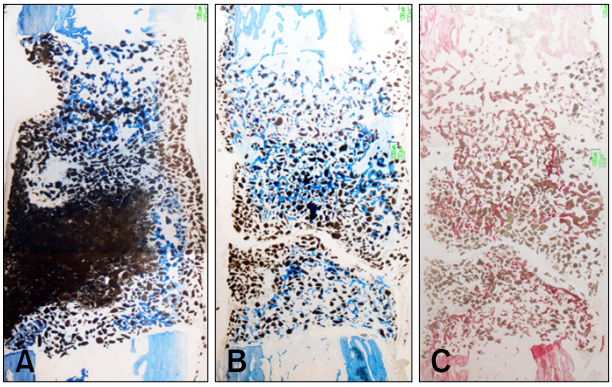

Fig. 3. Microphotographs of longitudinal sections of implants in the groups C (A) and CM (B, C) at 12 weeks after implantation of β-TCP. The proximal portion is at the top of the photomicrograph. The cranial aspect of bone (where the fixation plate had been) is at the left of photomicrograph. Bone appears blue or red, and ceramic appears black. (A, B) toluidine blue stain. (C) Villanueva-Goldner stain. ×10. Bone formation is observed around β-TCP throughout the implant. β-TCP remained in both side of the implant, especially under fixation plate and in the group C.

sections of implants in both groups 12 weeks after implantation (Fig. 3). β-TCP remained in both sides and the distal one third of the implant, especially under the fixation plate and in group C. Osteocytes were evident around the β-TCP (Fig. 4A). New bone was in direct contact with the β-TCP granules (Figs. 4B and C). Histomorphometric analysis revealed percentages of new bone formation in groups C and CM were 4.08 ± 2.08 and 10.92 ± 2.74, respectively ($p < 0.05$). Residual percentages of β-TCP were 40.63 ± 17.86 and 24.21 ± 8.75, in groups C and CM, respectively (Table 1).

Clinical application

Radiographically, increased opacity between radius and allograft bone, and a decreased radiolucent gap was checked four weeks after injection of canine UCB-MSCs. With time, the radiolucent site gradually decreased and the radiolucent fracture line disappeared (Fig. 5). Instability at fracture site

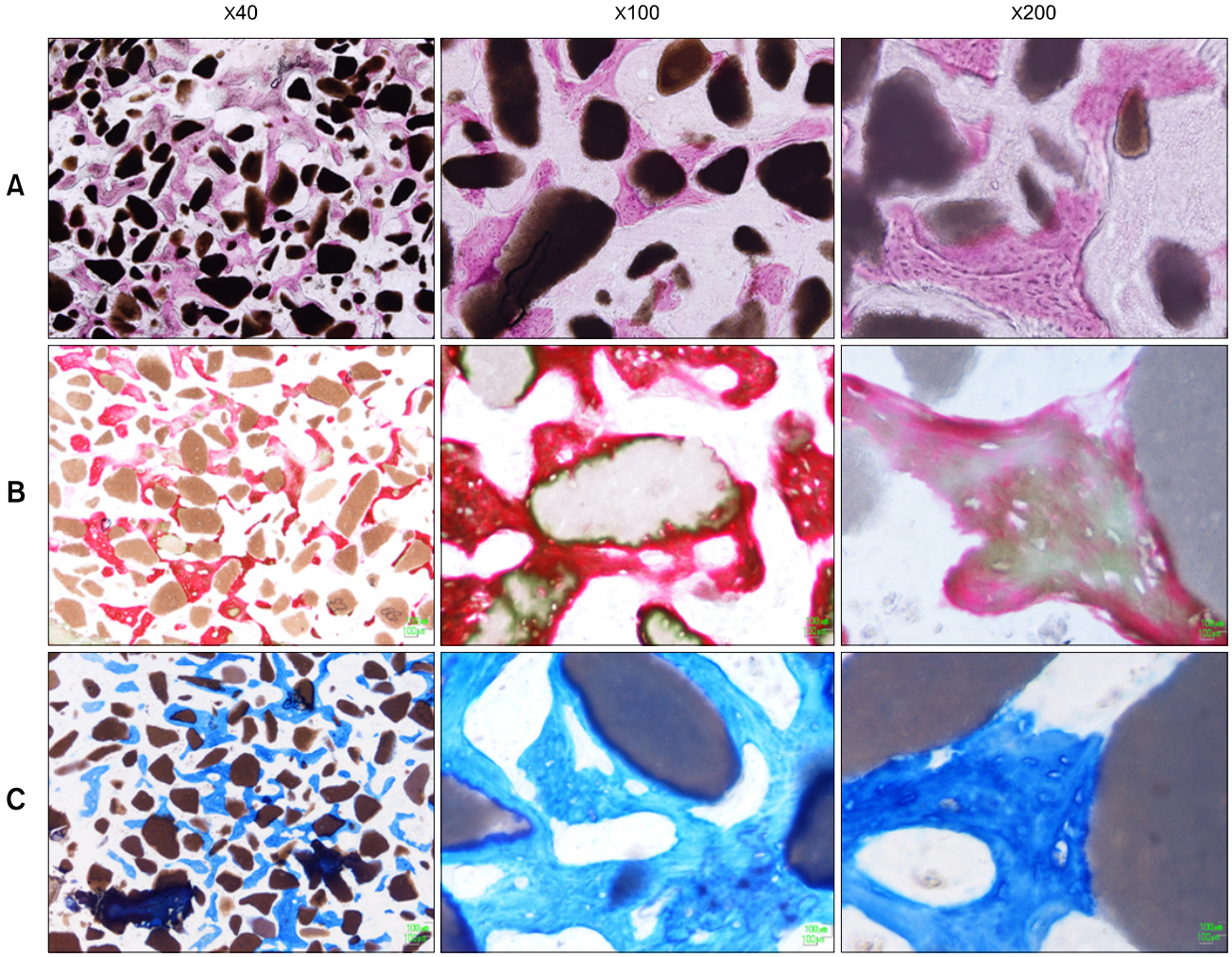

Fig. 4. Microphotographs of implants at 12 weeks after implantation in the group CM. New bone was in direct contact with the β-TCP granules. (A) H&E stain: Osteocyte is observed around the β-TCP. (B) Villanueva-Goldner stain (red-immature bone, green-mature bone). (C) Toluidine blue stain.

Table 1. Histomorphometric analysis

Group	NBA/TA (%)	RTA/TA (%)
C	4.08 ± 2.08[a]	40.63 ± 17.86
CM	10.92 ± 2.74*	24.21 ± 8.75

NBA: new bone formation area. RTA: residual β-TCP area. TA: total area. *$p < 0.05$ compared with C group. [a]All values are means ± SD.

Fig. 5. Lateral radiographs of antebrachium at 0, 4, 8, and 12 weeks after first injection of canine umbilical cord blood derived stem cells.

was decreased by 8 weeks after injection. The dog could bear weight partially by 8 weeks.

Discussion

Radiography is useful to assess the union at host bone-implant interfaces as an important factor of bone healing [1,3]. Presently, a distinct radiolucent zone at the interface between implants and the host bone was visible on the immediate postoperative radiographs. The absence of this radiolucent zone was considered to be an indication of union between the implant and the host bone. In the present study, union at the host bone-implant interface occurred more often and more rapidly in group CM than group C. An ideal bone graft substitute should resorb fully and at a predictable rate, while also providing a three-dimensional matrix to support bone ingrowth and ongrowth during resorption [33]. The appearance of implanted β-TCP on X-rays was the density of bone in early phase. Thereafter, as further resorption of the β-TCP and bone remodeling occurred, density decreased more [32]. In this study, radiolucency was found only near the bone end in group C, but throughout the entire graft in group CM at 12 weeks.

Previous studies used bloc ceramics with pores precultured with cells in osteogenic medium or vacuumed for uniform loading and retention of cells [13,34]. In the present study, β-TCP granules were mixed with cells immediately before implantation; this method of cell-matrix combination can be easily performed in a clinical setting.

In the previous report [3], new bone was distributed uniformly throughout the cell-matrix implant. However, in the present study, β-TCP remained in both sides and the distal one third of the implant, especially under the fixation plate and in group C, as evident histologically 12 weeks after implantation. β-TCP that remained under the fixation plate could be due to impaired blood supply to outer cortical bone beneath plates [8]. In the present study, implants were wrapped with TCP/PLGC membrane to prevent leakage of the β-TCP granule-cell mixture and invasion of fibrous connective tissues into the implant instead of vascular and host bone ingrowth. In assessing the present observations, it was suggested that vascular or bone ingrowth may have depended largely on proximal host bone. Bone formation with bone graft substitute relies on a complex sequence of events with a major dependence on vascular ingrowth, differentiation of osteoprogenitor cells, bone remodeling and graft resorption that occur together with host bone ingrowth into and onto the porous coralline microstructure or voids left behind during resorption [33]. Callus formation around an implant in the segmental defect treated with a ceramic cylinder that had been loaded with mesenchymal stem cells was reported [3]; similar observations were not made in the present study. It is conceivable that TCP/PLGC membrane might interrupt vascular ingrowth around implant and callus formation.

Histomorphological examinations conducted 12 weeks after the implantation of mixture of β-TCP and cells revealed significantly greater area of new bone formation than control ($p < 0.05$) and a smaller amount of residual TCP. Previous studies showed that bone marrow-derived MSCs are capable of forming bone *in vitro* [12,13], and when implanted in an appropriate matrix ectopically or orthotopically [3,14]. Implants with autologous bone marrow MSCs contain more new bones within and around implants in canine segmental bone defect [3]. While undifferentiated adipose derived stromal cells with β-TCP does not affect bone regeneration [20], canine UCB-MSCs presently produced a contrary result.

In a study involving athymic rats, human UCB-MSCs displayed osteogenic differentiation *in vitro*, survived after xenotransplantation and differentiated into osteoblasts that filled the bony defects [10]. A recent study reported that human UCB-MSCs have a significantly stronger osteogenic potential but less capacity in adipogenic differentiation than bone marrow MSCs *in vitro* [4]. Presently, canine UCB-MSCs might have enhanced new bone formation by differentiating to osteoblast progenitors. Alternatively, a paracrine effect of canine UCB-MSCs may have enhanced new bone formation. Analyses of bone marrow MSCs with real-time polymerase chain reaction and of bone marrow MSC-conditioned medium by antibody-based protein array

and enzyme-linked immunosorbant assay indicated that bone marrow MSCs secrete distinctively different cytokines and chemokines such as vascular endothelial growth factor (VEGF), insulin-like growth factor-1, epidermal growth factor, keratinocyte growth factor, angiopoietin-1, stromal derived factor-1, macrophage inflammatory protein-1alpha, -1beta and erythropoietin, compared to dermal fibroblasts [5]. Several cytokines, chemokines and growth factors are produced during *in vitro* osteogenic differentiation from human UCB-MSCs, with VEGF being perhaps the most critical driver of vascular formation during osteogenesis [26]. VEGF also stimulates osteoblast proliferation, migration and differentiation [23]. These cytokine alterations accelerate osteogenesis [16,19,30,35]. Further studies will be needed to elucidate the mechanism of bone formation by canine UCB-MSCs.

In a cortical allograft, the host-graft interface heals within 3 months [11]. Vascular invasion begins at the interface and progresses toward the center of the graft. Remodeling of the graft takes months to years, depending on the length, and might never be complete [24]. In the present clinical case, bone lysis and instability of the fractured site was evident by 9 weeks after cortical allograft. After injection of canine UCB-MSCs, bone regeneration gradually appeared in defect sites. Although there was some doubt whether bone formation was attributable to the introduced canine UCB-MSCs or to an endochondral sequence, the injected canine UCB-MSCs injected might play a role in osteoconduction in the graft site.

The results of the present study demonstrate that canine UCB-MSCs accelerate new bone formation upon the implantation of β-TCP into segmental defects in dogs. Implantation of allogenic UCB-MSCs with β-TCP holds promise in the clinical repair of segmental bone defects and non-union fractures.

Acknowledgments

The research was supported by the BK21 Program for Veterinary Science and Seoul R&BD Program (10548).

References

1. **Arinzeh TL, Peter SJ, Archambault MP, Van Den Bos C, Gordon S, Kraus K, Smith A, Kadiyala S.** Allogeneic mesenchymal stem cells regenerate bone in a critical-sized canine segmental defect. J Bone Joint Surg Am 2003, **85**, 1927-1935.
2. **Arinzeh TL, Tran T, Mcalary J, Daculsi G.** A comparative study of biphasic calcium phosphate ceramics for human mesenchymal stem-cell-induced bone formation. Biomaterials 2005, **26**, 3631-3638.
3. **Bruder SP, Kraus KH, Goldberg VM, Kadiyala S.** The effect of implants loaded with autologous mesenchymal stem cells on the healing of canine segmental bone defects. J Bone Joint Surg Am 1998, **80**, 985-996.
4. **Chang YJ, Shih DT, Tseng CP, Hsieh TB, Lee DC, Hwang SM.** Disparate mesenchyme-lineage tendencies in mesenchymal stem cells from human bone marrow and umbilical cord blood. Stem Cells 2006, **24**, 679-685.
5. **Chen L, Tredget EE, Wu PYG, Wu Y.** Paracrine factors of mesenchymal stem cells recruit macrophages and endothelial lineage cells and enhance wound healing. PLoS ONE 2008, **3**, e1886.
6. **Daculsi G.** Biphasic calcium phosphate concept applied to artificial bone, implant coating and injectable bone substitute. Biomaterials 1998, **19**, 1473-1478.
7. **Di Nicola M, Carlo-Stella C, Magni M, Milanesi M, Longoni PD, Matteucci P, Grisanti S, Gianni AM**. Human bone marrow stromal cells suppress T-lymphocyte proliferation induced by cellular or nonspecific mitogenic stimuli. Blood 2002, **99**, 3838-3843.
8. **Fossum TW, Hedlund CS, Johnson AL, Schulz KS, Seim HB, Willard MD, Bahr A, Carroll GL.** Small Animal Surgery. 3rd ed. pp. 930-1014, Mosby, St. Louis, 2007.
9. **Heise U, Osborn JF, Duwe F.** Hydroxyapatite ceramic as a bone substitute. Int Orthop 1990, **14**, 329-338.
10. **Jäger M, Sager M, Knipper A, Degistirici O, Fischer J, Kögler G, Wernet P, Krauspe R.** *In vivo* and *in vitro* bone regeneration from cord blood derived mesenchymal stem cells. Orthopade 2004, **33**, 1361-1372.
11. **Johnson AL, Stein LE.** Morphologic comparison of healing patterns in ethylene oxide-sterilized cortical allografts and untreated cortical autografts in the dog. Am J Vet Res 1998, **49**, 101-105.
12. **Kadiyala S, Jaiswal N, Bruder SP.** Culture-expanded, bone marrow-derived mesenchymal stem cells can regenerate a critical-sized segmental bone defect. Tissue Eng 1997, **3**, 173-185.
13. **Kadiyala S, Young RG, Thiede MA, Bruder SP.** Culture expanded canine mesenchymal stem cells possess osteochondrogenic potential *in vivo* and *in vitro*. Cell Transplant 1997, **6**, 125-134.
14. **Kasten P, Vogel J, Luginbühl R, Niemeyer P, Tonak M, Lorenz H, Helbig L, Weiss S, Fellenberg J, Leo A, Simank HG, Richter W.** Ectopic bone formation associated with mesenchymal stem cells in a resorbable calcium deficient hydroxyapatite carrier. Biomaterials 2005, 26, 5879- 5889.
15. **Kikuchi M, Koyama Y, Yamada T, Imamura Y, Okada T, Shirahama N, Akita K, Takakuda K, Tanaka J.** Development of guided bone regeneration membrane composed of beta-tricalcium phosphate and poly (L-lactide-co-glycolide-co-epsilon-caprolactone) composites. Biomaterials 2004, **25**, 5979-5986.
16. **Kitaura H, Nagata N, Fujimura Y, Hotokezaka H, Yoshida N, Nakayama K.** Effect of IL-12 on TNF-alpha-mediated osteoclast formation in bone marrow cells: apoptosis mediated by Fas/Fas ligand interaction. J Immunol 2000, **169**, 4732-4738.
17. **Koepp HE, Schorlemmer S, Kessler S, Brenner RE, Claes L, Günther KP, Ignatius AA.** Biocompatibility and osseointegration of beta-TCP: histomorphological and biomechanical studies in a weight-bearing sheep model. J

Biomed Mater Res B Appl Biomater 2004, **70**, 209-217.
18. **Kraus KH, Kirker-Head C.** Mesenchymal stem cells and bone regeneration. Vet Surg 2006, **35**, 232-242.
19. **Kwan Tat S, Padrines M, Théoleyre S, Heymann D, Fortun Y.** IL-6, RANKL, TNF-alpha/IL-1: interrelations in bone resorption pathophysiology. Cytokine Growth Factor Rev 2004, **15**, 49-60.
20. **Li H, Dai K, Tang T, Zhang X, Yan M, Lou J.** Bone regeneration by implantation of adipose-derived stromal cells expressing BMP-2. Biochem Biophys Res Commun 2007, **356**, 836-842.
21. **Lim JH, Byeon YE, Ryu HH, Jeong YH, Lee YW, Kim WH, Kang KS, Kweon OK.** Transplantation of canine umbilical cord blood-derived mesenchymal stem cells in experimentally induced spinal cord injured dogs. J Vet Sci 2007, **8**, 275-282.
22. **Lu J, Descamps M, Dejou J, Koubi G, Hardouin P, Lemaitre J, Proust JP.** The biodegradation mechanism of calcium phosphate biomaterials in bone. J Biomed Mater Res 2002, **63**, 408-412.
23. **Mayer H, Bertram H, Lindenmaier W, Korff T, Weber H, Weich H.** Vascular endothelial growth factor (VEGF-A) expression in human mesenchymal stem cells: autocrine and paracrine role on osteoblastic and endothelial differentiation. J Cell Biochem 2005, **95**, 827-839.
24. **Olmstead ML.** Small Animal Orthopedics. p. 150, Mosby, St. Louis, 1995.
25. **Oonishi H.** Orthopaedic applications of hydroxyapatite. Biomaterials 1991, **12**, 171-178.
26. **Penolazzi L, Lambertini E, Tavanti E, Torreggiani E, Vesce F, Gambari R, Piva R.** Evaluation of chemokine and cytokine profiles in osteoblast progenitors from umbilical cord blood stem cells by BIO-PLEX technology. Cell Biol Int 2008, **32**, 320-325.
27. **Rogers I, Casper RF.** Umbilical cord blood stem cells. Best Pract Res Clin Obstet Gynaecol 2004, **18**, 893-908.
28. **Sartoris DJ, Holmes RE, Resnick D.** Coralline hydroxyapatite bone graft substitutes: radiographic evaluation. J Foot Surg 1992, **31**, 301-313.
29. **Steffen T, Stoll T, Arvinte T, Schenk RK.** Porous tricalcium phosphate and transforming growth factor used for anterior spine surgery. Eur Spine J 2001, **10** (Suppl 2), S132- 140.
30. **Tang CH, Yang RS, Chen YF, Fu WM.** Basic fibroblast growth factor stimulates fibronectin expression through phospholipase C gamma, protein kinase C alpha, c-Src, NF-kappaB, and p300 pathway in osteoblasts. J Cell Physiol 2007, **211**, 45-55.
31. **Tseng SS, Lee MA, Reddi AH.** Nonunions and the potential of stem cells in fracture-healing. J Bone Joint Surg Am 2008, **90** (Suppl 1), 92-98.
32. **van Hemert WL, Willems K, Anderson PG, van Heerwaarden RJ, Wymenga AB.** Tricalcium phosphate granules or rigid wedge preforms in open wedge high tibial osteotomy: a radiological study with a new evaluation system. Knee 2004, **11**, 451-456.
33. **Walsh WR, Chapman-Sheath PJ, Cain S, Debes J, Bruce WJM, Svehla MJ, Gillies RM.** A resorbable porous ceramic composite bone graft substitute in a rabbit metaphyseal defect model. J Orthop Res 2003, **21**, 655-661.
34. **Wang J, Asou Y, Sekiya I, Sotome S, Orii H, Shinomiya K.** Enhancement of tissue engineered bone formation by a low pressure system improving cell seeding and medium perfusion into a porous scaffold. Biomaterials 2006, **27**, 2738-2746.
35. **Xu LX, Kukita T, Kukita A, Otsuka T, Niho Y, Iijima T.** Interleukin-10 selectively inhibits osteoclastogenesis by inhibiting differentiation of osteoclast progenitors into preosteoclast-like cells in rat bone marrow culture system. J Cell Physiol 1995, **165**, 624-629.